ELSEVIER

Biophysical Chemistry 109 (2004) 333–344

Biophysical Chemistry

www.elsevier.com/locate/bpc

Changes in drug ^{13}C NMR chemical shifts as a tool for monitoring interactions with DNA☆

Eilis A. Boudreau[1], István Pelczer[2], Philip N. Borer[3], Gregory J. Heffron[4], Steven R. LaPlante[5,*]

[1]*Health Science Research and Development Program, Portland VA Medical Center, Portland, OR 97239, USA*
[2]*Department of Chemistry, Princeton University, Princeton, NJ 08540, USA*
[3]*Department of Chemistry, Syracuse University, Syracuse, NY 13244-1200, USA*
[4]*Department of Biological Chemistry and Molecular Pharmacology, Harvard Medical School, 240 Longwood Avenue, Boston, MA 02115, USA*
[5]*Boehringer Ingelheim (Canada) Ltd., Research and Development, 2100 Cunard St., Laval, P.Q., Canada H7S 2G5*

Received 11 November 2003; received in revised form 11 November 2003; accepted 11 December 2003

Abstract

The antibiotic drug, netropsin, was complexed with the DNA oligonucleotide duplex $[d(GGTATACC)]_2$ to monitor drug ^{13}C NMR chemical shifts changes. The binding mode of netropsin to the minor groove of DNA is well-known, and served as a good model for evaluating the relative sensitivity of ^{13}C chemical shifts to hydrogen bonding. Large downfield shifts were observed for four resonances of carbons that neighbor sites which are known to form hydrogen bond interactions with the DNA minor groove. Many of the remaining resonances of netropsin exhibit shielding or relatively smaller deshielding changes. Based on the model system presented here, large deshielding NMR shift changes of a ligand upon macromolecule binding can likely be attributed to hydrogen bond formation at nearby sites.

Keywords: Netropsin; Ligand; Nuclear magnetic resonance (NMR); Deoxyribo nucleic acid (DNA); Drug; Chemical shift; Carbon; Inhibitor

Abbreviations: A, adenosine; T, thymidine; G, guanosine; C, cytidine; nmr, nuclear magnetic resonance; H-bond, hydrogen bond; δ, chemical shift; $\Delta\delta$, change in chemical shift; T_m, melting temperature; Net, netropsin; ppm, parts per million

☆ The oligonucleotide discussed in this article has no terminal phosphates unless specifically denoted.

*Corresponding author. Tel.: +1-450-6824640; fax: +1-450-6828434.
E-mail address: slaplante@lav.boehringer-ingelheim.com (S.R. LaPlante).

0301-4622/04/$ - see front matter © 2003 Elsevier B.V. All rights reserved.
doi:10.1016/j.bpc.2003.12.005

1. Introduction

^{13}C NMR chemical shifts are very sensitive to changes in the environment of carbon nuclei, which should make it a practical, atomic-level parameter for monitoring drug interacts with target nucleic acids. This would require, however, a better understanding of the relative sensitivity of ^{13}C chemical shifts to various binding events such as formation of hydrogen bonds (H-bonds), dehydration, changes in torsion angles, and base stacking or packing. Previous investigations shed light into the relative sensitivity of NMR chemical shifts in a nucleic acid environment. Early studies monitored changes in chemical shifts upon duplex formation in model oligonucleotides. ^{1}H NMR studies on single- and double-stranded oligonucleotides indicate that almost all the base protons are shielded as temperature is decreased through the transition from the random coils to base-stacked structures [1–4]. Likewise, ^{13}C NMR studies of r(AAA) and r(AAG), both of which lack a hydrogen-bonded duplex structure, indicate that all the base carbons become shielded upon decreasing the temperature [5]. Such changes have been attributed to the gain of ring current shielding [6], and additionally for ^{13}C, an increase in steric contact between the stacked bases [5]. For several DNA oligonucleotide duplexes, we observed that most of the base carbons exhibit similar (shielding) chemical shifts upon lowering the temperature from the random coils [7,8]. Surprisingly, approximately 25% of the base carbons exhibited large (approx. 1 ppm) deshielding changes upon duplex formation; this was attributed to making Watson-Crick H-bonds. Furthermore, ^{13}C NMR studies of RNA di- and trinucleotides [5,9] and DNA oligonucleotides [7,10,11] have monitored chemical shifts as a function of changes in sugar pucker. The major factor affecting chemical shifts was attributed to sugar pucker changes while other factors apparently contribute to a smaller extent.

The well-characterized system of netropsin binding to the minor groove of DNA oligonucleotides [12–22] allows for further exploration of the relationship between drug ^{13}C chemical shifts changes and the predominant interactions upon DNA binding. It is known that netropsin binds sequence specifically to double stranded DNA, requiring at least four contiguous A–T base pairs for maximal binding strength. Several sources including H-bonding are responsible for the specificity and binding of netropsin. Dickerson and coworkers reported from crystallographic data that netropsin H-bonds to the TO2 and AN3 sites in its complex with the dodecamer duplex $[d(CGCGAATTCGCG)]_2$ [23,24]. They proposed that water binds in the minor groove of A–T regions of B-DNA in a 'spine of hydration', and as many as 12 of these water molecules are displaced from the dodecamer duplex upon binding of netropsin. Sugar pucker changes were also reported for the interaction of netropsin to DNA oligonucleotides. Dickerson and coworkers [12,17] showed crystallographic data on the sugar pucker changes of $[d(CGCGAATTCGCG)]_2$ upon interaction with netropsin. Changes in the ^{1}H NMR [13] and ^{13}C [25,26] and ^{15} N NMR [25,27] chemical shifts were also monitored for DNA oligonucleotide binding to netropsin. Distinct changes in ^{13}C and ^{15} N chemical shifts of the bases were attributed to H-bonding, and changes in ^{13}C chemical shifts of the sugars were sensitive to sugar pucker changes.

In this work, we investigate the relation between changes in ^{13}C NMR shifts of netropsin upon binding to the DNA duplex $[d(GGTATACC)]_2$ as a model system. Netropsin (Fig. 1a) is known to bind to the minor groove of the 'TATA' central portion of the DNA duplex (Fig. 1b) and form H-bonds to AN3 and TO2 (Fig. 1c).

2. Materials and methods

2.1. NMR experiments applied for ^{13}C resonance assignments of free netropsin

One-dimensional ^{1}H and ^{13}C spectra of free netropsin in DMSO-d_6 and D_2O solvents were acquired on a General Electric GN-500 spectrometer (500.13 MHz proton frequency) using a 5 mm $^{1}H/^{13}C$ dual probe. Samples in DMSO-d_6 solvent consisted of 20 mM netropsin, and samples in D_2O solvent consisted of a saturated concentration of netropsin (given the presence of a precipitant in this solvent, the concentration was not

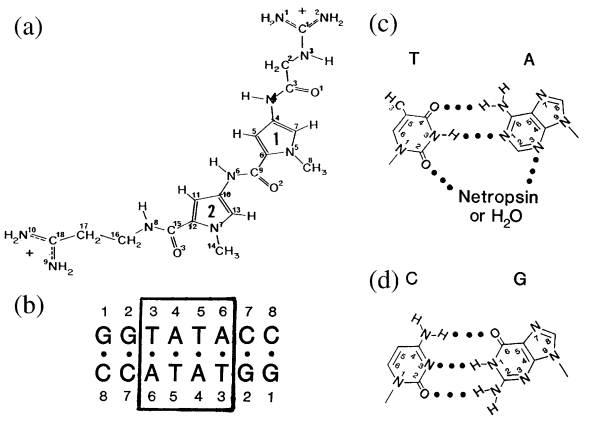

Fig. 1. (a) The molecular formula and numbering scheme for netropsin is shown. (b) Numbering scheme for the self-complementary duplex $[d(GGTATACC)]_2$. The boxed in portion of the duplex is the binding site of netropsin. (c) Water/Na+ and netropsin H-bond sites on the A-T base pairs are shown. (d) A representation of the C-G base pair.

known). The later sample also contained 100 mM NaCl and 10 mM sodium cacodylate. Proton spectra were collected with a spectral width of 5000 Hz and 16K data points. Carbon and APT spectra were collected with spectral widths of 32 000 Hz, 16K data points, a recycle time of 2 s, and an average of 400 scans. ^{13}C chemical shifts were referenced to the methyl carbon resonance of sodium cacodylate at 20.11 ppm. One-dimensional ^{13}C spectra were also collected on samples containing various ratios of D_2O/DMSO solvent ranging from 100% D_2O to 90% DMSO-d_6.

One-dimensional NOE difference experiments were acquired on the D_2O sample using the following pulse sequence: relax-$\{\beta$-$\Delta\}_n$-recovery-read pulse/acquisition. The small-flip-angle pulse (β) was tuned to be line-selective, and a DANTE pulse train was inserted for presaturation of the residual solvent peak. The first sideband at lower field from the carrier was used for saturation. The interpulse delay (Δ) was successively varied in a time averaged cycle, and four on- and off-resonance spectra were acquired. The overall saturation time for each irradiation was 5 s, while a 10 ms recovery time was inserted prior to the read pulse and data acquisition to obtain more distortion-free results. Each FID was an average of 256 scans and 16K data points.

Long-range $^1H-^{13}C$ J-coupling connectivities were determined with the assistance of one-dimensional $^1H-^{13}C$ INEPT and two-dimensional $^1H-^{13}C$ correlation experiments. The INEPT experiments included selective proton pulses (INAPT). The two-dimensional $^1H-^{13}C$ correlation experiments (carbon detection) were performed on a DMSO-d_6 sample consisting of 210 mM netropsin and 100 mM NaCl. Three experiments were run to establish single and multiple bond connectivities using delays that were optimized for coupling constant values of 125, 30 and 8 Hz. The following parameters were used for data collected on the GN-500 spectrometer: 5814 and 30 303 Hz spectral widths for the F1 (^1H) and F2 (^{13}C) dimensions, 2K points in the ^{13}C dimension, 128 t_1 increments, relaxation delay of 1.2 s, and 888 averaged scans for each FID. The following parameters were used for data collected on the WB-360 spectrometer using a 10 mm carbon selective probe: 3594 Hz and 13 888 Hz spectral widths for F1 and F2, a time domain data size of $8K \times 256$ points, a relaxation delay of 2 s, and 256 scans per FID. Chemical shifts were referenced to the methyl carbon of DMSO-d_6 at 39.50 ppm.

Two-dimensional $^1H-^{13}C$ correlation experiments (proton detection) were also performed on a D_2O sample and run on a Bruker AMX-400 (400.13 MHz) instrument using a 5 mm inverse geometry probe. Both single HMQC and multiple bond HMBC correlations were acquired. In each case, the spectral widths in F2 and F1 were 5050 Hz and 18 545 Hz, respectively. The data matrix in the time domain was $4K \times 512$ points with TPPI quadrature detection in t_1 for the HMQC experiment. The HMBC experiment was presented in absolute value mode. For each FID, 256 scans were averaged. Relaxation delay was set to 1.5 s. All experiments were acquired at 30 °C temperature.

Two-dimensional ROESY experiments were run on the DMSO-d_6 sample at 500 MHz (GN-500 spectrometer) using a 5 mm inverse geometry probe (Cryomagnets, Inc.), with spectral width of 5650 Hz in both dimensions. The data size was 4K and 256 points in t_2 and t_1, and a States-

Haberkorn-Ruben (SHR) acquisition scheme was used to acquire a double-block file. The mixing time was 150 ms with a spin-locking field of 7 kHz and 32 scans per each t_1 increment. Chemical shifts were referenced to the residual methyl protons of DMSO at 2.49 ppm.

2.2. NMR experiments applied for ^{13}C resonance assignments of netropsin in the complex

$[d(GGTATACC)]_2$ was synthesized from phosphoramidites using the syringe method [28] and purified from shorter chain length impurities by C_8 reverse-phase HPLC using tetrabutylammonium acetate as an ion-pairing buffer in CH_3CH/H_2O gradients. The 8-mer was then purified from salts, i.e. tetrabutylammonium acetate, using a Sephadex A-25 column. The column was pre-equilibrated with 0.01 M cacodylate solution, the sample was loaded, washed with five column volumes of 0.1 M NaCl solution, and then eluted with 1 M NaCl solution. The excess NaCl was removed from the 8-mer using a Sephadex G-10 column with distilled water as the solvent.

Netropsin (Serva Fine Biochemicals) was added to an 5 mm NMR tube containing the DNA oligonucleotide $[d(GGTATACC)]_2$ (7 mM in duplex, 14 mM in single strands) and 0.1 M NaCl, 10^{-4} M EDTA, 10 mM cacodylate pH 7.2, 20% D_2O in a total volume of 0.5 ml. Netropsin was added incrementally to the duplex and spectra recorded at drug: duplex ratios of 0.1, 0.2, 0.33, 0.5, 0.67, 1.0 and 1.5. Spectra at several temperatures were measured at ratios of 0.2, 0.5 and 1.0 (three different samples were used). Natural abundance spectra were taken at 125.8 MHz for ^{13}C and 500 MHz for ^{1}H using a 5 mm dual probe on a General Electric GN-500. Unless otherwise indicated, the spectra were taken at 23 °C. For the ^{13}C spectra, a one pulse experiment was used with a 90° pulse, repetition rates of 3 s and 'MLEV' decoupling. 10 000–12 000 transients were averaged with 16 k data tables (8 k real + 8 k imaginary) and sweep width of 30 kHz. The ^{1}H spectra were recorded in aqueous solution using the Jump-Return experiment to suppress the H_2O peak [29]. ^{13}C spectra were referenced to the cacodylate peak at 20.11 ppm. ^{1}H spectra were referenced to the H_2O peak at 4.75 ppm. Assignment of the netropsin resonances in the complex were secured by comparison of spectra taken at various ligand: DNA ratios and temperatures along with comparisons with spectra of free duplex and free netropsin. This assignment strategy took advantage of the incremental shifting of resonances due to the fast exchange binding nature of the complex (on the NMR time scale). Assignment of the ^{13}C resonances of $[d(GGTATACC)]_2$ in complex with netropsin have been previously reported [25,26].

3. Results and discussion

3.1. Nomenclature

Specific atoms of netropsin will be referred to using the numbering scheme given in Fig. 1. Specific carbons of the DNA oligonucleotide will be referred to using an abbreviated form where the base type is designated first by letter, the chain position second, and the carbon class last. For example, G2,8 represents carbon number eight in the guanine base of the second residue from the 5′-end of $[d(GGTATACC)]_2$, whereas TC6 designates the class: thymine carbon six. If another type of atom is being discussed, the atom type will be designated, for example G2,H8.

3.2. ^{13}C chemical shift assignments of netropsin

The resonance assignments of netropsin in the free and bound states proved to be a significant challenge given many issues encountered. The relatively low solubility of free netropsin in aqueous buffer resulted in low signal intensity, thus alternative approaches were required. Furthermore, the close chemical symmetry of this compound resulted in some resonance proximity and overlap. Given this issue, it was decided to first assign the ^{1}H and ^{13}C resonances of free netropsin in DMSO solvent, in which netropsin is highly soluble. This afforded the convenience of higher signal-to-noise data and the possibility of applying numerous experiments for solving the symmetry-related issues. Such resonance proximity or overlap is evident in the ^{13}C spectrum in Fig. 2 of netrospin in D_2O solvent (i.e. see the regions between 122

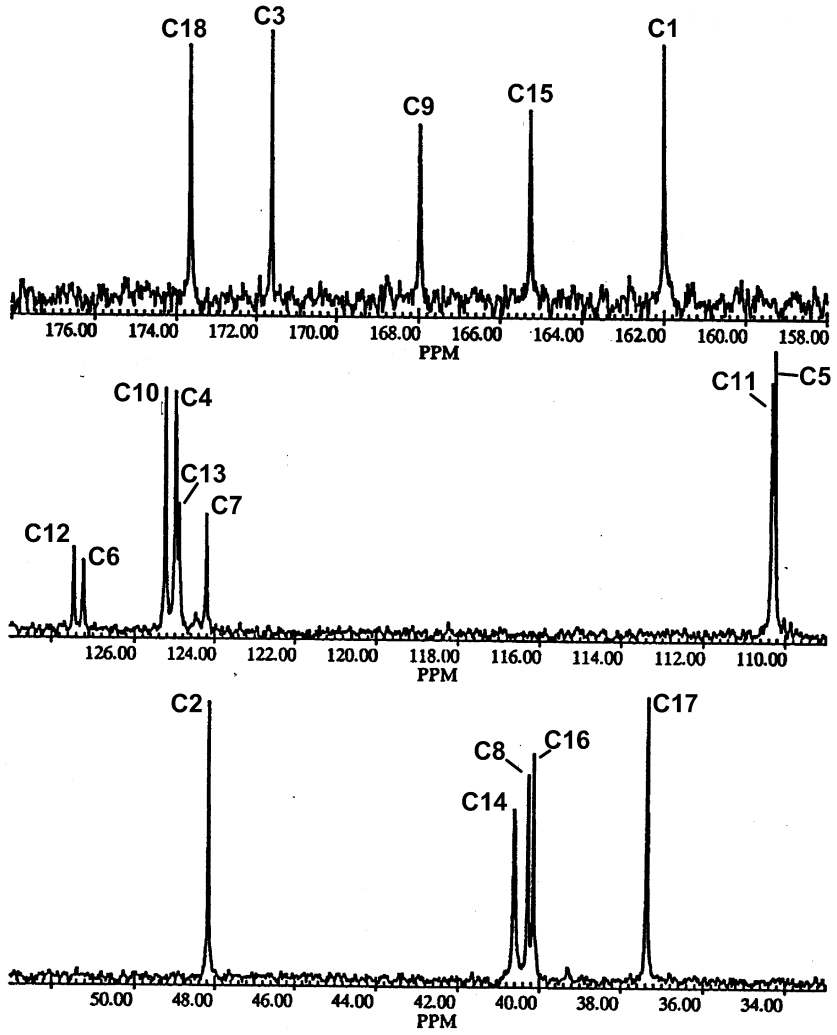

Fig. 2. High resolution ^{13}C NMR spectrum of free netropsin in D_2O.

and 127 ppm, near 110 ppm, and between 41 and 40 ppm). The ^{1}H (Fig. 3a) and ^{13}C (Table 1) resonance assignments in DMSO-d_6 were straightforward using a battery of experiments (e.g. ROESY data in Fig. 3A and $^{1}H-^{13}C$ correlation data in Fig. 3b) along with various conditions as described in the Section 2.

Similar experiments were also applied to help secure the ^{1}H and ^{13}C (Table 1) resonance assignments in D_2O solvent. Limitations in applying these experiments due to low solubility and signal-to-noise were supplemented by spectral comparison strategies. The strategies included the careful comparisons of one-dimensional and correlation spectra taken at numerous D_2O/DMSO-d_6 solvent ratios. Any remaining ambiguities were resolved by taking spectra at different temperatures. The resonance assignments in aqueous buffer were easily secured by one-dimensional ^{13}C spectral comparisons with spectra acquired in D_2O solvent. Differences in chemical shifts are likely due to the effect of salt in the buffer.

The ^{13}C resonance assignments of netropsin when bound to $[d(GGTATACC)]_2$ (Fig. 4) were

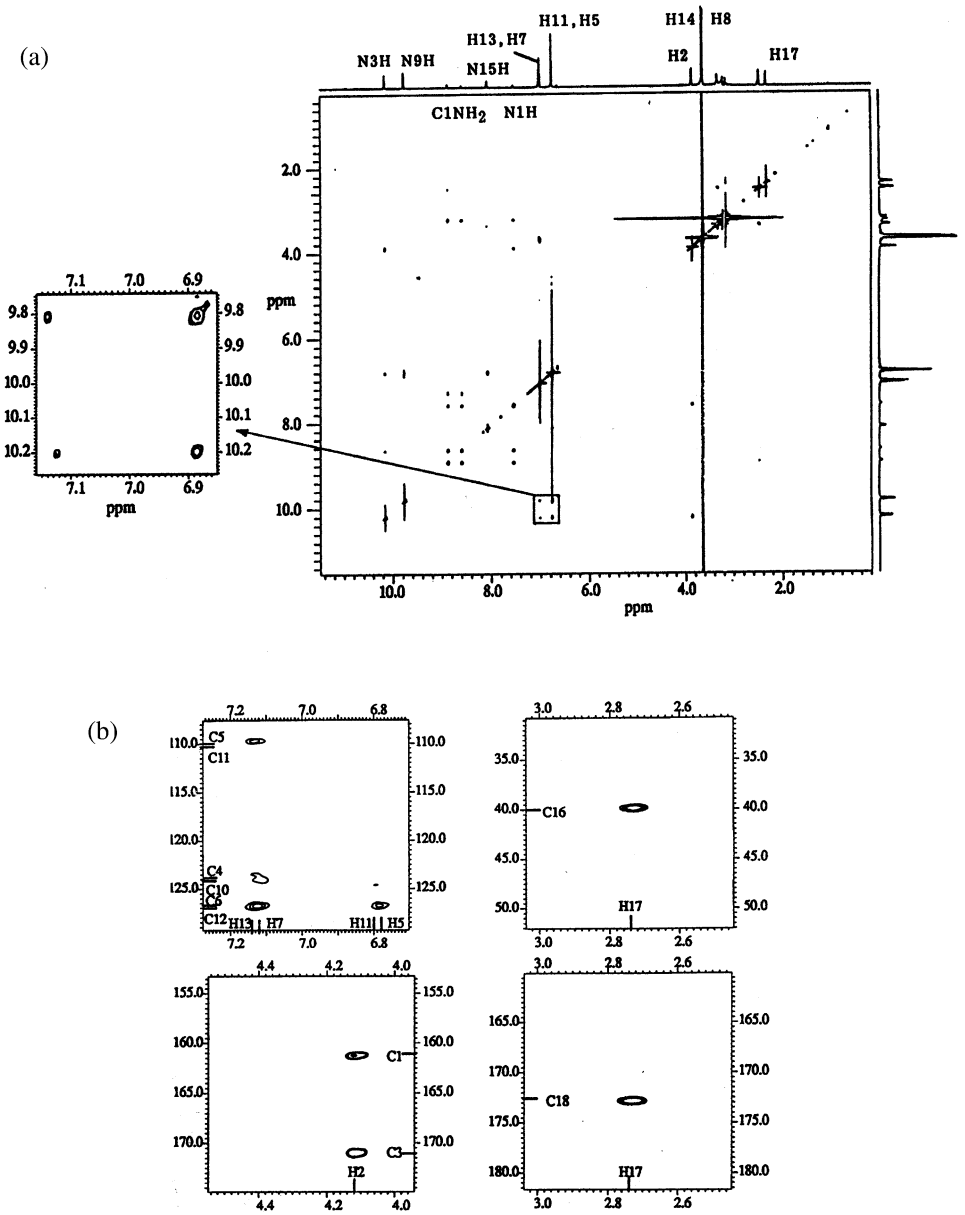

Fig. 3. (a) ROESY spectrum with an inset showing correlations between N3H and N9H, and H13, H7, H11, and H5. A t_1 noise ridge at ca. 3.2 ppm was removed from the spectrum during processing. The H16 peak was buried in the noise ridge on the diagonal. The $C18NH_2$ resonances are not shown on this spectrum because of their weak intensity but are located at ca. 6.5 ppm. (b) Selected correlation regions from the HMBC spectrum showing assignments of C1, C3, C4, C5, C6, C10, C11, C12, C16 and C18.

secured by comparing one-dimensional spectra in which netropsin was added incrementally to the duplex and spectra recorded at various drug:duplex ratios and temperatures. This assignment method (by direct comparison of spectra) has been successful [26] and was also possible here because

Table 1
^{13}C NMR resonance assignments of free netropsin in D_2O and DMSO-d_6 solvents

Assignment	δ (ppm) D_2O	δ (ppm) DMSO-d_6
C18	173.67	169.25
C3	171.62	164.41
C9	167.98	161.41
C15	165.27	158.34
C1	162.01	157.88
C12	127.47	122.98
C6	127.25	122.47
C10	125.22	122.06
C4	124.89	121.34
C13	124.82	118.34
C7	124.21	118.31
C11	110.33	104.78
C5	110.25	104.03
C2	48.18	44.06
C14	40.63	36.32
C8	40.29	36.56
C16	40.17	36.25
C17	37.38	32.88

the resonances moved as average peaks as the netropsin concentration or the temperature was increased, a phenomenon that is typical for fast exchange binding (on the NMR time scale). Assignment of the ^{13}C resonances of [d(GGTATACC)]$_2$ in complex with netropsin have been previously reported [25,26] using a combination of heretonuclear correlation experiments [30,31] and the spectral comparison methods [8,10].

3.3. Changes in ^{13}C chemical shifts of netropsin upon binding [d(GGTATACC)]$_2$

The lowest-field portion of the 125.8 MHz ^{13}C NMR spectra of the [d(GGTATACC)]$_2$ duplex, free netropsin, and the complex are shown in Fig. 4a, b and c, respectively. This part of the spectra contains nearly all of the quaternary DNA and netropsin carbons, including the carbonyls and amino-bonded carbons that could potentially be involved in hydrogen-bonds in the complex. Most of the resonances are well resolved, and given the

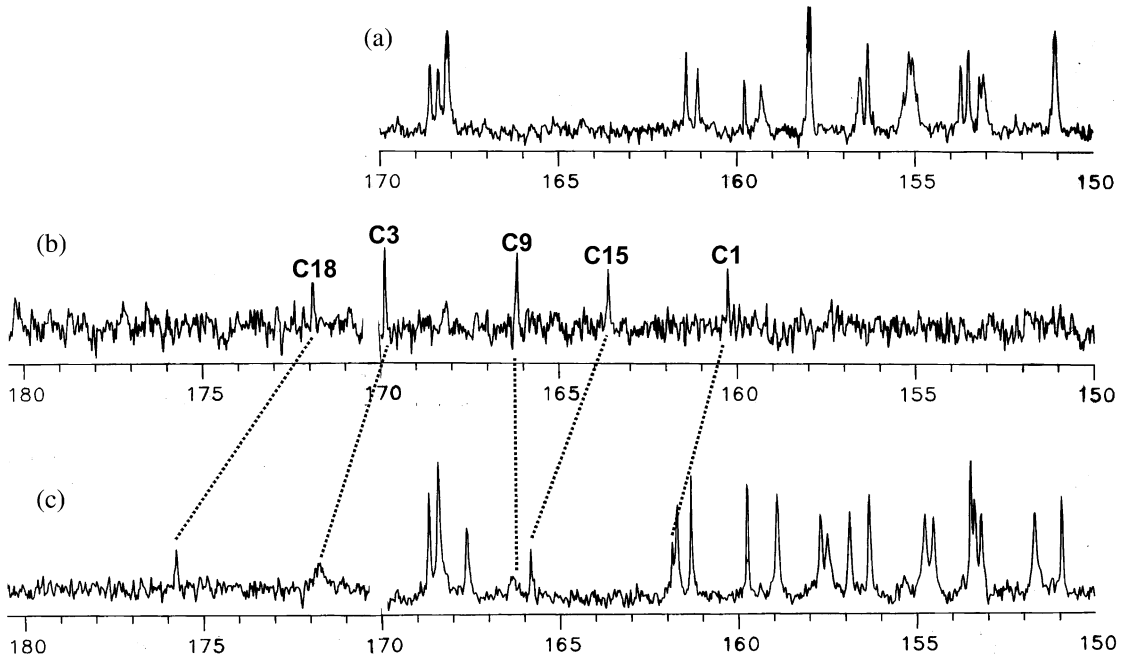

Fig. 4. (a) ^{13}C NMR spectra of the lowest field base carbons of free [d(GGTATACC)]$_2$, (b) ^{13}C NMR spectra of free netropsin, and (c) ^{13}C NMR spectra of the 1: 1 complex of [d(GGTATACC)]$_2$ with netropsin.

Table 2
Changes in ^{13}C NMR resonances of netropsin upon binding to [d(GGTATACC)$_2$]

Resonance assignment	$\Delta\delta$ (ppm)[a]
C18	−3.9
C3	−1.9
C9	−0.1
C15	−2.1
C1	−1.7
C12	Between 0.7 and 1.3[b]
C6	Between 0.7 and 1.3[b]
C10	Between −0.2 and −2.2[c]
C4	Between −0.2 and −2.2[c]
C13	Between −0.2 and −2.2[c]
C7	Between −0.2 and −2.2[c]
C11	Between 1.0 and 1.6[b]
C5	Between 1.0 and 1.6[b]
C2	0.4
C14	Between 0.0 and −0.9[b]
C8	Between 0.0 and −0.9[b]
C16	Between 0.0 and −0.9[b]
C17	−0.7

[a] $\Delta\delta$ is the chemical shift (ppm) in the free state minus the chemical shift in the bound state.

[b] Due to resonance overlap or other reasons, the exact change in chemical could not be determined. However, the change is at or within the range shown.

[c] Due to resonance overlap or other reasons, the exact change in chemical could not be determined. However, the change is at or within the range shown. Inspection of the spectra suggest that three resonances change very little and one changes significantly.

fast exchange nature of the complex the netropsin assignments in the complex could be determined.

Fig. 4b and c show that four netrospin resonances experience large downfield shifts (move left to higher ppm values) upon binding the DNA duplex. Interesting, one of the netropsin resonances in Fig. 4 experiences little to no change. A quantitative summary of these changes and those from the other regions of the ^{13}C spectra are given in Table 2. Unfortunately, not all of the resonance assignment ambiguities could be resolved for the netropsin resonances in the upfield regions, and only ranges of shift changes could be confidently provided. Of these upfield resonances, it is interesting to note that most changes in chemical shift upon DNA binding are either small or upfield changes.

3.4. Hydrogen bonding effects on DNA base ^{13}C chemical shifts in the DNA environment

Previous studies found that ^{13}C resonances of DNA are highly sensitive to structural changes (e.g. strand association upon double helix formation). Large deshielding changes upon duplex association from single strands have been attributed to carbons that are bonded to heteroatoms involved in Watson-Crick H-bonds [7]. Large shielding and smaller shift changes for some carbon resonances were attributed to other structural events such as steric compression and base stacking (ring currents).

3.5. H-bonding and netropsin: [d(GGTATACC)]$_2$

We reported that upon complex formation with netropsin, there were no large changes in chemical shifts for the DNA base guanine and cytosine, and notably large changes for the bases thymidine and adenosine [26]. These observations confirmed that netropsin binds to the A–T rich center of [d(GGTATACC)]$_2$. A large negative $\Delta\delta$ deshielding occurred for AdoC4 (−0.64 ppm). Since each resonance represents a carbon from each strand, two H-bonds were identified. Hydrogen bonding at DNA AdoN3 sites required that netropsin was physically binding in the duplex minor groove.

In that study, the clear majority of the large $\Delta\delta$ values for the DNA duplex, upon complexation, occurred at T5 in the central base pairs of the complex, illustrated in Fig. 5. The large shielding $\Delta\delta$ values observed could not be explained by formation of H-bonds to nearby covalent-bonded heteroatoms (large deshielding would have been expected). This suggested that the positive $\Delta\delta$ of T5,2 may be the result of breaking a H-bond with solvent water upon netropsin displacement of the ‘spine of hydration’. This in turn would disrupt the water’s role (Fig. 5a) in constraining the A–T pairs in their natural propeller twisted state. Insignificant changes in DNA shifts were attributed to

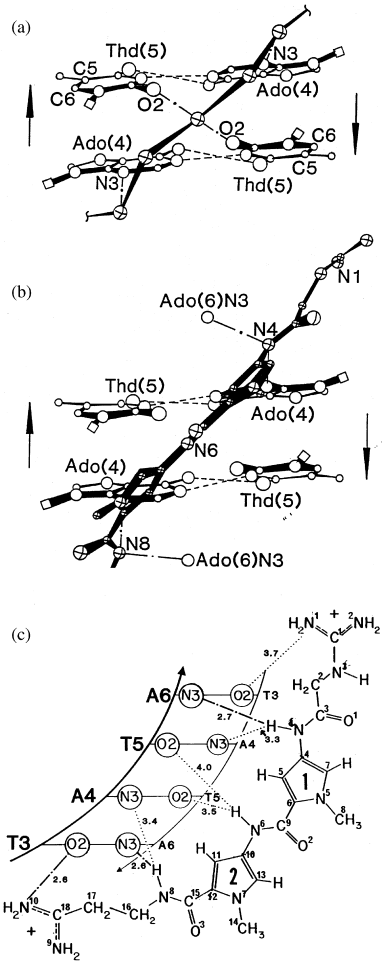

Fig. 5. A view into the minor groove of the central 5′ApT3′ step in $[d(GGTATACC)]_2$, showing (a) a portion of the spine of hydration which binds specifically to ThdO2 and AdoN3 (oxygen atoms of the water molecules or Na+ are illustrated as cross-hatched circles), and (b) a bound netropsin molecule (cross-hatched circles). The two ends of netropsin are slightly different, producing an asymmetric complex. Netropsin N6 is too distant from TO2 to form classical hydrogen bonds. Netropsin N4 and N8 should form bifurcated H-bonds to A4 and A6 N3 atoms, and netropsin N10 should H-bond to T3,2O based on consideration of the X-ray model for the netropsin: $[d(CGCGAATTCGCG)]_2$ complex. Both duplexes have the central ApT step in common, although the other residues are different; it is assumed here that the TO2/AN3 H-bond sites in the minor groove are nearly isomorphous. The C1′ atoms are indicated as squares; otherwise the diameter of the circles indicates the type of atom, increasing in the order: C, N, O. Arrows show the 5′–3′ direction of the chains. (c) Distances (Å) are shown.

replacing a H-bond to water with one to netropsin, and to magnetic environment changes.

Upon complexation, most ^{13}C resonances of netropsin and $[d(GGTATACC)]_2$ experience at least small changes in chemical shift. These changes in netrospin resonances likely arise from changes in dynamic behavior of netropsin upon binding DNA (torsion angle changes) and/or due to changes in magnetic environment from the phosphate groups. Large effects on ^{13}C chemical shifts due to ring current of the DNA bases are unlikely. Distances from the center of the netropsin pyrrole ring to A and T base carbons were determined by molecular graphics to be greater than 4.5 Å with most in the range of 5–6 Å. At these distances and considering the angular dependence of the ring current effect, none of the carbons should be affected by more than 0.1 ppm [32,33].

It is interesting that large deshielding $\Delta\delta$ are observed (Table 2) for the netropsin resonances of C18, C3, C15, and C1 upon complexation with of $[d(GGTATACC)]_2$. These changes suggest that H-bonds were formed at the neighboring sites (NH2 of 9 and 10), amide (HN4 or O=C3), the amides (H–N9 or O=C15), and at NH2 (1 and 2) or H–N3. These data are consistent with the model of the complex based on an X-ray structure (described below). Also, it is interesting that H–N3's neighbor C2 experiences a 0.4 shielding $\Delta\delta$ is consistent with H-bonding at NH2 (1 and 2) rather than at H–N3. Our X-ray based model (Fig. 5) is consistent with this and with H-bonding to H–N8 and H–N4. This would suggest that the −2.2 and −0.9 deshielding $\Delta\delta$ could arise from the neighboring C4 and C16 sites, although the assignment of these resonances remains unresolved for the time being. Finally, the lack of large $\Delta\delta$ involving the H–N6/O=C9 amide and its neighbors is consistent with lack of H-bond formation with this amide. Again, this is in agreement with the X-ray based model and ^1H NMR studies (see below).

3.6. Comparison with X-ray and ^1H NMR data of the bases

Dickerson's laboratory has proposed that water binds in the minor groove of A–T regions of B-

DNA in a 'spine of hydration' [23,24]. This model has been recently revised based upon a very high resolution X-ray structure that shows an inner spine composed of Na+ ions and water, and an outer spine of water [34–36]. From X-ray data, Dickerson's work indicates that netropsin displaces as many as 12 of the water/Na+ in the inner spine; the spine components bind to each other, TO2, and AN3 [12,17,24]. Fig. 5a shows the central two base pairs in the duplex [d(CGCG-AATTCGCG)]$_2$ and the oxygens (or Na+) of five of the waters in the spine. TO2 and AN3 are nearly isomorphous in a regular B-DNA geometry, so any sequence of A–T pairs allows the spine to form; at least four contiguous A–T pairs are required for netropsin to bind with maximum strength. Fig. 5b shows that netropsin displaces the specifically bound waters/Na+ and that its amide nitrogens are located in similar positions to the water oxygens (or Na+) in Fig. 5a. The pyrrole rings conflict sterically with the adenine bases, forcing netropsin N6 to be approximately 3.7 Å from the H-bond acceptors at T5,O2; this is too distant to form H-bonds. Patel and Shapiro [14,15] also report from ^{1}H-NOESY data that the netropsin pyrrole protons are in close contact with the AH2 protons of [d(GGTATACC)]$_2$. They and others [27] further suggest that these close contacts rule out the presence of water/Na+ molecules being sandwiched between the netropsin and [d(GGTATACC)]$_2$ at the binding site. In our study, a large positive $\Delta\delta = 1.36$ ppm at T5,2 of [d(GGTATACC)]$_2$ is consistent with loss of a H-bond with water/Na+ and lack of formation of a H-bond with netropsin at the T5,O2 sites.

The Dickerson model shows that the outer netropsin amides (N4 and N8) should form short H-bonds to A6,N3 which are likely the source of the deshielding effect for C15 and C3 observed in our data. It is also consistent with the large deshielding values of -2.2 and -0.9 corresponding to C4 and C16, respectively, although definitive assignments to these residues remains unresolved. Patel and Shapiro [15] state that in rapid exchange netropsin would unbind and jump rapidly between two states, the one shown in Fig. 5b and one where N1 is at the lower left. Therefore, both sets of terminal amides of netropsin would be involved in H-bonds to DNA, which would be consistent with our observation of large deshielding shifts of C1 and C18 in this work. Furthermore, the lack of large deshielding $\Delta\delta$ for C9 is also consistent with DNA:netropsin data [15,16,23,24,26]. C9 of netropsin is covalently neighboring N6, which fails to form a significant H-bond to the DNA minor groove.

4. Conclusion

The experiments described here were designed to explore the effects of H-bonding on the carbon chemical shifts of netropsin upon binding to DNA. Based on this model system, the results suggest that ^{13}C NMR spectroscopy may provide a technique for identifying the sites of drugs that are involved in H-bonds. In conclusion, changes in ligand ^{13}C shifts may be an additional design parameter for monitoring details of drug interactions with macromolecules.

Acknowledgments

We thank Drs M. Bös and P. Anderson for encouragement and support. We also appreciate experimental support from Dr Graham Jackson.

References

[1] P.N. Borer, L.S. Kan, P.O.P. Ts'o, Conformation and interaction of short nucleic acid double-stranded helices. I. Proton magnetic resonance studies on the non-exchangeable protons of ribosyl ApApGpCpUpU, Biochemistry 14 (1975) 4847–4863.

[2] P. Cruz, E. Bubienko, P.N. Borer, A model for base overlap in RNA, Nature (London) 298 (1982) 198–200.

[3] D.M. Cheng, L.S. Kan, E.E. Leutzinger, K. Jayaraman, P.S. Miller, P.O.P. Ts'o, Conformational study of two short pentadeoxyribonucleotides, CpCpApApG and CpTpTpGpG, and their fragments by proton NMR, Biochemistry 21 (1982) 621–630.

[4] S. Tran-Dinh, J. Taboury, J.M. Neumann, T. Huynh-Dinh, B. Genissel, B.L. d'Estaintot, et al., Proton NMR and circular dichroism studies of the B and Z conformations of the self-complementary deoxyhexanucleotide d(m5C-G-C-G-m5C-G): mechanism of the Z-B-coil transitions, Biochemistry 23 (1984) 1362–1371.

[5] M.P. Stone, S.A. Winkle, P.N. Borer, Carbon-13 NMR of ribosyl ApApA, ApApG and ApUpG, J. Biomol. Struct. Dyn. 3 (1986) 767–781.

[6] C. Giessner-Prettre, B. Pullman, On the atomic or 'local' contributions to proton chemical shifts due to the anisotropy of the diamagnetic susceptibility of the nucleic acid bases, Biochem. Biophys. Res. Commun. 70 (1976) 578–581.

[7] P.N. Borer, S.R. LaPlante, N. Zanatta, G.C. Levy, Hydrogen-bonding effects and ^{13}C-NMR of the DNA double helix, Nucleic Acids Res. 16 (1988) 2323–2332.

[8] S.R. LaPlante, E.A Boudreau, N. Zanatta, G.C. Levy, P.N. Borer, J. Ashcroft, et al., Carbon-13 NMR of the bases of three DNA oligonucleotide duplexes: assignment methods and structural features, Biochemistry 27 (1988) 7902–7909.

[9] P.P. Lankhorst, C. Erkelens, C.A.G. Haasnoot, C. Altona, Carbon-13 NMR in conformational analysis of nucleic acid fragments. Heteronuclear chemical shift correlation spectroscopy of RNA constituents, Nucleic Acids Res. 11 (1983) 7215–7230.

[10] S.R. LaPlante, N. Zanatta, A. Hakkinen, A.H.-J. Wang, P.N. Borer, ^{13}C-NMR of the deoxyribose sugars in four DNA oligonucleotide duplexes: assignment and structural features, Biochemistry 33 (1994) 2430–2440.

[11] X. Xiao-Ping, A.K. Wing-Lok, S.C.F. Au-Yeung, Chemical shift and structure relationship in nucleic acids: correlation of backbone torsion angles and with 13C chemical shifts, J. Am. Chem. Soc. 120 (1998) 4230–4231.

[12] M.L. Kopka, C. Yoon, D. Goodsell, P. Pjura, R.E. Dickerson, The molecular origin of DNA-drug specificity in netropsin and distamycin, Proc. Natl. Acad. Sci. USA. 82 (1985) 1376–1380.

[13] D.J. Patel, Antibiotic-DNA interactions: intermolecular nuclear Overhauser effects in the netropsin-d(C-G-C-G-A-A-T-T-C-G-C-G) complex in solution, Proc. Natl. Acad. Sci. USA 79 (1982) 6424–6428.

[14] D.J. Patel, L. Shapiro, Molecular recognition in noncovalent antitumor agent-DNA complexes: NMR studies of the base and sequence dependent recognition of the DNA minor groove by netropsin, Biochimie 67 (1985) 887–915.

[15] D.J. Patel, L. Shapiro, Sequence-dependent recognition of DNA duplexes: netropsin complexation to the TATA site of the d(G-G-T-A-T-A-C-C) duplex in aqueous solution, Biopolymers 25 (1986) 707–727.

[16] D.J. Patel, L. Shapiro, Sequence-dependent recognition of DNA duplexes. Netropsin complexation to the AATT site of the d(G-G-A-A-T-T-C-C) duplex in aqueous solution, J. Biol. Chem. 261 (1986) 1230–1240.

[17] M.L. Kopka, C. Loon, D. Goodsell, P. Pjura, R.E. Dickerson, Binding of an antitumor drug to DNA. Netropsin and C-G-C-G-A-A-T-T-BrC-G-C-G, J. Mol. Biol. 183 (1985) 553–563.

[18] H. Lida, G. Jia, J.W. Lown, Rational recognition of nucleic acid sequences, Curr. Opin. Biotechnol. 1 (1999) 29–33.

[19] D.E. Wemmer, Designed sequence-specific minor groove ligands, Ann. Rev. Biophys. Biomol. Struct. 29 (2000) 439–461.

[20] D. Rentzeperis, L.A. Marky, T.J. Dwyer, B.H. Geierstanger, J.G. Pelton, D.E. Wemmer, Interaction of minor groove ligands to an AAATT/AATTT site of thermodynamic characterization and solution structure, Biochemistry 34 (1995) 2937–2945.

[21] W.H. Gmeiner, W. Cui, D.E. Konerding, P.A Keifer, S.K. Sharma, A.M. Soto, et al., Shape-selective recognition of a model Okazaki fragment by geometrically-constrained bis-distamycins, J. Biomol. Struct. Dyn. 3 (1999) 507–518.

[22] J. Feigon, W.A. Denny, W. Leupin, D.R. Kearns, Interactions of antitumor drugs with natural DNA: ^{1}H NMR study of binding mode and kinetics, J. Med. Chem. 4 (1984) 450–465.

[23] H.R. Drew, R.E. Dickerson, Structure of a B-DNA dodecamer. III. geometry of hydration, J. Mol. Biol. 151 (1981) 535–556.

[24] M.L. Kopka, A.V. Fratini, H.R. Drew, R.E. Dickerson, Ordered water structure around a B-DNA dodecamer. A quantitative study, J. Mol. Biol. 163 (1983) 129–146.

[25] J. Ashcroft, D.H. Live, D.J. Patel, D. Cowburn, Heteronuclear two-dimensional nitrogen-15 and carbon-13 NMR studies of DNA oligomers and their netropsin complexes using indirect proton detection, Biopolymers 31 (1991) 45–55.

[26] S.R. LaPlante, P.N. Borer, Changes in ^{13}C-NMR chemical shifts of DNA as a tool for monitoring drug interactions, Biophys. Chem. 90 (2001) 219–232.

[27] Y. Rhee, C. Wang, B.L. Gaffney, R.A. Jones, Nitrogen-15-labeled oligodeoxynucleotides. 6. Use of nitrogen-15 NMR to probe binding of netropsin and distamycin to {d[CGCGAATTCGCG]}2, J. Am. Chem. Soc. 115 (1993) 8742–8746.

[28] T. Tanaka, R.L. Letsinger, Syringe method for stepwise chemical synthesis of oligonucleotides, Nucleic Acids Res. 10 (1982) 3249–3260.

[29] P. Plateau, M. Gueron, Exchangeable proton NMR without base-line distorsion, using new strong-pulse sequences, J. Am. Chem. Soc. 104 (1982) 7310–7311.

[30] S.R. LaPlante, J. Ashcroft, D. Cowburn, G.C. Levy, P.N. Borer, Carbon-13 NMR assignments of the protonated carbons of [d(TAGCGCTA)]2 by two-dimensional proton-detected heteronuclear correlation, J. Biomol. Struct. Dyn. 5 (1988) 1089–1099.

[31] J. Ashcroft, S.R. LaPlante, P.N. Borer, D. Cowburn, Sequence specific carbon-13 NMR assignment of non-protonated carbons in [d(TAGCGCTA)]2 using proton detection, J. Am. Chem. Soc. 111 (1989) 363–365.

[32] E. Becker, High Resolution NMR, Academic Press, New York, 1980, p. 73.

[33] C. Giessner-Prettre, B. Pullman, P.N. Borer, L.S. Kan, P.O.P. Ts'o, Ring-current effects in the NMR of nucleic acids: a graphical approach, Biopolymers 15 (1976) 2277–2286.

[34] X. Shui, L. McFail-Isom, G.G. Hu, L.D. Williams, The B-DNA dodecamer at high resolution reveals spine of water on sodium, Biochemistry 37 (1998) 8341–8355.
[35] N.V. Hud, V. Sklenar, J. Feigon, Localization of the ammonium ions in the minor groove of DNA duplexes in solution and the origin of DNA A-tract bending, J. Mol. Biol. 286 (1999) 651–660.
[36] N.V. Hud, J. Feigon, Localization of divalant metal ions in the minor groove of DNA A-tracts, J. Am. Chem. Soc. 119 (1997) 5756–5757.